Methods for Radioactive Source Localization via Uncrewed Aerial Systems

Caleb J. Adams

Thesis submitted to the Faculty of the

Virginia Polytechnic Institute and State University

in partial fulfillment of the requirements for the degree of

Master of Science

in

Mechanical Engineering

Kevin B. Kochersberger, Chair

Mark Pierson

Alireza Haghighat

February 15, 2024

Blacksburg, Virginia

Keywords: UAS, Radiation Detection, Autonomous Localization

Methods for Radioactive Source Localization via Uncrewed Aerial Systems

Caleb J. Adams

(ABSTRACT)

Uncrewed aerial systems (UAS) have steadily become more prevalent in both defense and industrial applications. Nuclear detection and deterrence is one such field that has given rise to many new opportunities for UAS operations. There is a need to research and develop methods to integrate existing radiation detection technology with UAS capable of flying low-altitude missions. This low-altitude scanning can be achieved by combining small and lightweight radiation detectors and state-of-the-art aircraft and avionics. High resolution mapping can then be conducted using the results of these scans.

Significant work has been conducted in this field by both private industry and academic institutions, including the Uncrewed Systems Lab (USL) at Virginia Tech. This work seeks to expand this body of knowledge and provide practical experimental information to showcase and validate the efficacy of radiation detection via UAS. Multiple missions were conducted using samples of ^{137}Cs and ^{60}Co as a radioactive source. Various filtering methods were applied to the results of these missions to produce visual maps that aid in the localization of an unknown source to compare various flight parameters. In addition, significant work was conducted to characterize two radiation detectors available to the USL to provide metrics to assist in the UAS design and flight planning. Finally, the detectors were taken to Savannah River National Laboratories to conduct experiments to provide information to aid future designs and missions that wish to detect a wider variety of radioactive sources.

Methods for Radioactive Source Localization via Uncrewed Aerial Systems

Caleb J. Adams

(GENERAL AUDIENCE ABSTRACT)

Drones are becoming more common in many applications for both industry and defense. One of these applications is in the field of nuclear detection which seeks to both regulate the shipping of radioactive material as well as aid response to nuclear disasters. Methods need to be researched to combine existing radiation detectors with new drone technology. These new state-of-the-art drones are capable of flying at very low altitudes which can allow for the use of small and lightweight radiation detectors.

Past work in this area, including at the Uncrewed Systems Lab (USL) at Virginia Tech, has explored larger scale aircraft as well as simulated radioactive sources. This work expands the existing knowledge of this field by providing scan results from real radioactive sources and drone flights. Multiple search flights were conducted using small quantities of radioactive cesium and cobalt. Maps were then produced using the information from these flights to showcase the system's ability to quickly locate the areas of high radioactivity. Flights were flown with different altitudes and speeds to determine the effects on mapping accuracy. Finally, experiments were conducted at Savannah River National Laboratories on a variety of more controlled nuclear materials to help inform future drone designs and mission planning.

Dedication

To my wife, my parents, and my friends for all of their love and support.

H-O-K-I-E-S Hokies!

Contents

List of Figures

List of Tables

List of Abbreviations

CBP Customs and Border Protection

cps counts per second

GPS Global Positioning System

MCA Multichannel Analyzer

NSDD National Nuclear Security Administration's Office of Nuclear Smuggling Detection and Deterrence

PMT Photo-multiplier Tube

RPM Radiation Portal Monitor

RSS Received Signal Strength

SRNL Savannah River National Laboratory

sUAS Small Uncrewed Aerial System

UAS Uncrewed Aerial System

USL Uncrewed Systems Laboratory

Chapter 1

Introduction

Each year millions of dollars and thousands of man-hours are spent on both the research and implementation of methods to detect and deter illegitimate transportation of nuclear material. The National Nuclear Security Administration's Office of Nuclear Smuggling Detection and Deterrence (NSDD) works to coordinate international efforts to detect and limit the shipping and transportation of controlled nuclear materials. In 2018, this office received data from over 800 radiation portal monitors (RPMs) which scanned or searched roughly 70 million occupants [3]. Figure 1.1 shows the distribution of this data according to the type of RPM.

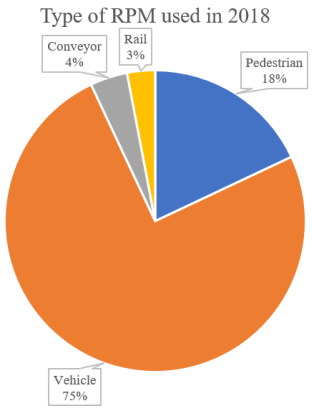

Figure 1.1: Distribution of RPM type used in 2018

From this data it is apparent that the majority of occupants being scanned are vehicles. Approximately 50 million vehicles or containers transported by vehicle were scanned in 2018. While the vast majority of these vehicles are able to be scanned and searched at stationary

RPMs located at strategic bottleneck points in shipping lanes, a significant number of vehicles are still manually searched with handheld radiation detectors. In addition, at many locations all alarms provided by the RPMs are then investigated by operators with handheld detectors to verify the readings and conduct a more thorough search.

Recent advancements in uncrewed aerial system (UAS) technology provide an excellent opportunity for researchers and industry professionals to develop automated radiation search systems to assist in the detection and localization of controlled nuclear material. Additionally, systems like these could be used to autonomously and remotely map affected areas after any nuclear disasters to mitigate the exposure human operators would encounter when conducting emergency response and cleanup. There have been significant developments in radiation monitoring via drones in this field, particularly after the Fukushima nuclear disaster in 2011 [15]. Since then, several international agencies and private companies have begun development into remote sensing and mapping systems to more effectively respond to potential future nuclear disasters as well as provide more granular inspection data to help prevent accidents altogether.

This work exists to build upon previous efforts made in this field of study by both researchers at Virginia Tech and other institutions. Specifically, this paper focuses on the development of a platform capable of performing autonomous radiation scans as well as methods to process the collected data and determine source location. The following sections outline the work done regarding both of these topics as well as providing recommendations regarding future research that should be conducted in this field.

Chapter 2

Literature Review

This section exists to review prior work on this topic as well as to establish basic understanding of relevant topics. The field of radiation detection and measurement is well developed, and the basic concepts and physics are discussed here. This section will also provide an overview of the work done specifically regarding localization of radioactive material and establish the importance of continued research in this area.

2.1 Localization Methods

Signal source localization has been important for both military and commercial uses since the invention of radio transmissions in the late 1800's [4]. One example of very early signal localization was a type of beamforming used extensively by the German Luftwaffe in World War II. By using a system called the "Knickebein", they were able to guide bombers in the dark of night using multiple radio beams that intersected over the intended bombing targets[8]. In more recent years, wireless sensor networks and global positioning systems (GPS) have become necessary for countless systems in industry, transportation, and defense. There are several methods and algorithms that have been developed to facilitate these systems, and there are two main categories that are discussed here:

1. Triangulation based on time-of-arrival (ToA) and time-difference-of-arrival (TDoA)
2. Localization based on received signal strength (RSS)

Whatever method that is used, there are two variables that must be determined in order to perform localization: direction and distance from source. There are several methods that can be used to measure these two variables. One method often used in acoustic localization is to use time of arrival to determine the direction of a source.

By implementing an array of microphones at different locations, it is possible to use the different times of arrival to triangulate a source's originating direction. This is very useful in the field of acoustic localization since the speed of sound in air is approximately 340 m/s. Because this speed is relatively slow when compared to the sampling frequency of modern microphones, an array with modest spacing between sensors can provide very accurate directional information in addition to distance. Unfortunately, gamma radiation travels much faster - at the speed of light, nearly 300,000,000 m/s - which makes this method impractical for this project due to the extraordinary requirements on equipment speed and accuracy.

Another possible method to determine direction of arrival of a signal is to use received signal strength (RSS) in conjunction with an array of sensors. This is discussed in part by Brennan et al. in regards to using distributed sensor networks in order to detect a moving radioactive source. Their research with Los Alamos National Laboratory showed that a network of distributed sensors could detect radioactive sources in moving vehicles in a way that was comparable to portal monitors [5]. By using multiple sensors in known locations, the relative RSS's could be compared to the measured background levels in order to flag vehicles that contained controlled materials for further inspection. Brennan's work involved the use of 11 sensors located in arrays surrounding a roadway.

In contrast, this paper involves a single sensor that is then flown to different locations while the source remains stationary. The goal is not only detection in this case, but also source localization. This changes the problem slightly and removes the requirement of fast detection, but the basic variables (direction and distance) must still be determined. In fact,

these variables must be determined at many points and produce a single localization based upon the data collected. This data processing can be accomplished via several methods which have been explored in similar research.

2.2 Prior Development on Localization Methods

There has been significant research done in the field of radiation detection and mapping via uncrewed rovers and aircraft. Of particular interest to this work is the collection of past research conducted by members of the Uncrewed Systems Lab at Virginia Tech.

In their work, Towler explored and developed two localization methods that they identified as being possibly effective for radiation detection and localization. Through rigorous simulations, Towler compared a grid-based recursive Bayesian estimator against a contour analysis [16]. He found that while both algorithms performed well, the contour analysis algorithm in particular could be implemented in a fashion which would provide fully autonomous capabilities when implemented into a UAS.

He was able to prove through simulation that this method could locate multiple sources very accurately. A major limitation of this method is that, for large sources, the contour following could take a very long time and use a significant portion of the flight time of the UAS he was designing for [16]. This led to his additional work in developing optimized ingress and egress flight plans.

Prior to Towler, Brewer also explored the use of various algorithms and laid the groundwork for Towler's exploration of those algorithms. His work largely pertained to a Bayesian particle swarm filtering method to locate a simple simulated point source. [7]. In addition to developing his algorithm for this localization, Brewer conducted flights with a simulated

source to display the implementation of this type of search algorithm into a real UAS.

Both Brewer and Towler worked with the USL Yamaha RMAX helicopter [7]. This UAS is capable of carrying a very large payload of up to 28 kg (61 pounds) [16]. While this immense carrying capacity is impressive, it presents constraints for both mission practicality and safety in ways that a much smaller UAS does not. The USL has recently developed a significantly smaller platform capable of flying a notably different mission profile and has led to this work.

2.3 Recent Developments in UAS-Based Radiation Scanning

It is worth mentioning several of the recent developments and research conducted in this specific area. One example of this is work done by researchers at Pacific Northwest National Laboratory. A comparison was made between extremely low-flying UAS (under one meter, typically) and human operator carried detectors. They concluded that this type of system had "good potential" but will require further advancements in UAS instrumentation to fully replace human operators. [6]

A similar group of researchers at Pacific Northwest National Laboratory continued in this research with their work titled "Drones for Decommissioning". This work expanded on the previously mentioned ultra-low testing at extremely slow speeds (0.2 m/s) and continued the comparison with human based radiation detection. [9] They determined that human operators and UAS based systems conducted radiation scans very similarly in the context of decommissioning areas used in nuclear development, testing, and industry. Once again, these researchers recommend that this is a promising result but further development and tuning

will be required before this type of system is fully adopted for decommissioning purposes at extremely low altitudes. [9]

Another sector of radiation detection that UAS can benefit is that of disaster response and monitoring. The International Atomic Energy Agency (IAEA) references their use of UAS based systems in their response plan and assistance during the Fukushima accident in 2011. [14] In 2012, the IAEA in conjunction with the Fukushima Prefecture began implementing UAS based detection systems into their radiological monitoring program following the disaster.

As UAS technology develops, the IAEA expects expanded use of these systems in disaster response and monitoring. Critically, this new method of radiation monitoring will protect human operators from exposure, as well as allow for less expensive long-term observation of affected areas. The IAEA is currently conducting research and training to expand the capabilities and use of these systems for future disaster response scenarios. [14]

Chapter 3

Background

The field of radiation detection and measurement is well developed, and the basic concepts and physics are discussed here. Specifically, the gamma ray interactions and sensing instrumentation that are relevant to this study are important information for later chapters and overall understanding.

3.1 Overview of Radiation Detection

This section exists in order to establish a basic understanding of the physics, technology, and methods of detecting and characterizing radioactive materials. This background information is necessary to this project as well as any future work related to this field.

3.1.1 Gamma Radiation

While there are several forms of radiation that result from the decay of radioactive isotopes that can be used for detection, the focus of this paper is solely on gamma rays and their detection. This is mainly due to the detection hardware available to the USL for testing, as well as the relative ease of acquiring sample radioactive sources.

Gamma rays are generally produced following two types of events: beta decay and nuclear reactions [11]. Both modes of gamma ray production create identical rays but at different

energy levels. The gamma rays produced by nuclear reactions typically possess much higher levels of energy when compared to those gamma rays released following beta decay. While nuclear reactions can be used to produce very high energy gamma rays, this effect is hard to produce and requires complex equipment and lab conditions. Therefore this type of gamma ray production was not considered for this project.

Gamma rays produced following beta decay possess lower energy characteristics than those from a nuclear reaction and are much easier to produce. There are many gamma ray emitting isotopes that are commonly used in laboratory testing. Some of the most common sources are ^{60}Co, ^{137}Cs, ^{57}Co, and ^{22}Na. These sources are preferred due to their relatively long half-lives as well as the easily recognizable nature of their gamma ray emissions. The sources used for in-flight testing in this thesis are discussed in 3.2.2 Radioactive Sources and consist of ^{137}Cs and ^{60}Co. Of these, ^{137}Cs is the primary source used in this work and it's decay scheme is shown in Figure 3.1 [11][12].

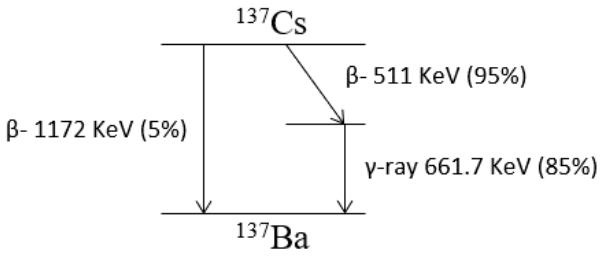

Figure 3.1: Cs-137 Decay Scheme

Radioactive sources are often modeled as point sources emitting energy equally in all direction. This is especially true for the small and nearly spherical sources used in this study. Due to these sources being omnidirectional and isotropic emitters, the radiation field forms a sphere for any given intensity level.

This means that these sources and the associated radiation follow the inverse square law which can be used to describe the decrease in intensity as a function of distance from the

source. This relationship is illustrated in Figure 3.2 and shown mathematically in Equation 3.1 where I is the intensity of the source at a given radius r and the source strength at its surface is S. This information is useful to model radioactive sources in simulations of radiation scans, which Brewer utilized this his work on this topic. [7]

$$I = \frac{S}{4\pi r^2} \tag{3.1}$$

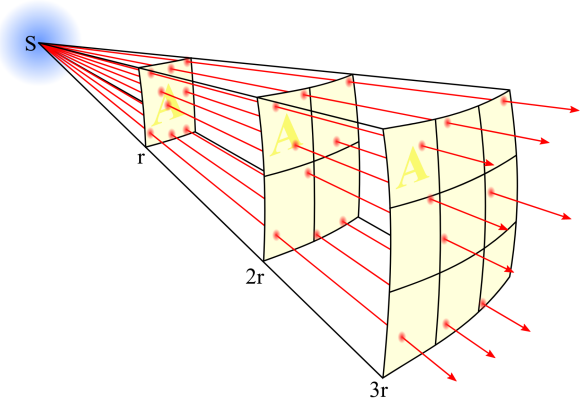

Figure 3.2: Inverse Square Law

Figure by user Borb. Use is licensed under CC BY-SA 3.0

3.1.2 Radiation Detectors

There are several types of radiation detectors commonly used to detect and identify gamma ray emitting isotopes.

- Ionization Chambers
- Proportional Counters
- Geiger-Müller Counters
- Scintillation Detectors
- Solid-State or Semiconductor Detectors

Each of these types of detectors is capable of detecting gamma ray radiation, but due to the mission constraints only two of these are viable options for this project. Weight and size are critical requirements, as well as the ability to interface with the onboard computer installed on the UAS. Additionally, the ability to perform gamma ray spectroscopy is immensely valuable once detection has been achieved and isotope identification is desired.

These restrictions narrowed the viable options to scintillation detectors and solid-state detectors as they are the most compact options, as well as the only two options that allow for spectral analysis in addition to raw counting. [11]

Due to equipment availability and ease of integration, NaI(Tl) scintillation detectors were chosen for this project. The USL at Virginia Tech has access to several of these detectors of varying size that are available for testing.

NaI Scintillation Detector Overview

Scintillation detectors (specifically with NaI(Tl) crystals) are some of the most common instruments used in large scale radiation detection. They are often favored for field applications due to being relatively inexpensive, durable, and reliable. There is a large amount of literature that exists on the physics and interactions that enable these types of detectors to operate. [11] For the purposes of this work, only the general characteristics of the detectors are required knowledge.

NaI(Tl) scintillation detectors use the luminescent properties of the NaI(Tl) crystal to determine when a gamma-ray interaction occurs. As the incoming radiation loses energy in the crystal a small amount of light is released. This light is then amplified using a photo-multiplier tube (PMT) and converted to electrical signals that can then be read and interpreted as information on the radiation that interacted with the crystal. [11]

Because the amplitude of the signal relates directly with the energy of the incoming radiation, these types of detectors can be used for both the counting of radiation as well as gamma spectroscopy. Gamma spectroscopy is the field of determining what the radioactive source is that produces the incoming gamma rays. This makes scintillation detectors very useful in deterrence/defense applications in which the identity of an unknown nuclear material must be quickly determined. This project does not directly investigate spectroscopy for isotope identification, but the gamma spectrum was considered when performing background subtraction (as the majority of background radiation is located at lower energies than those that are produced by radioisotopes). [11] An example spectrum was collected using a 2"x2" NaI(Tl) detector with a 138 μCi source tested at Savannah River National Laboratories and is shown in Figure 3.3.

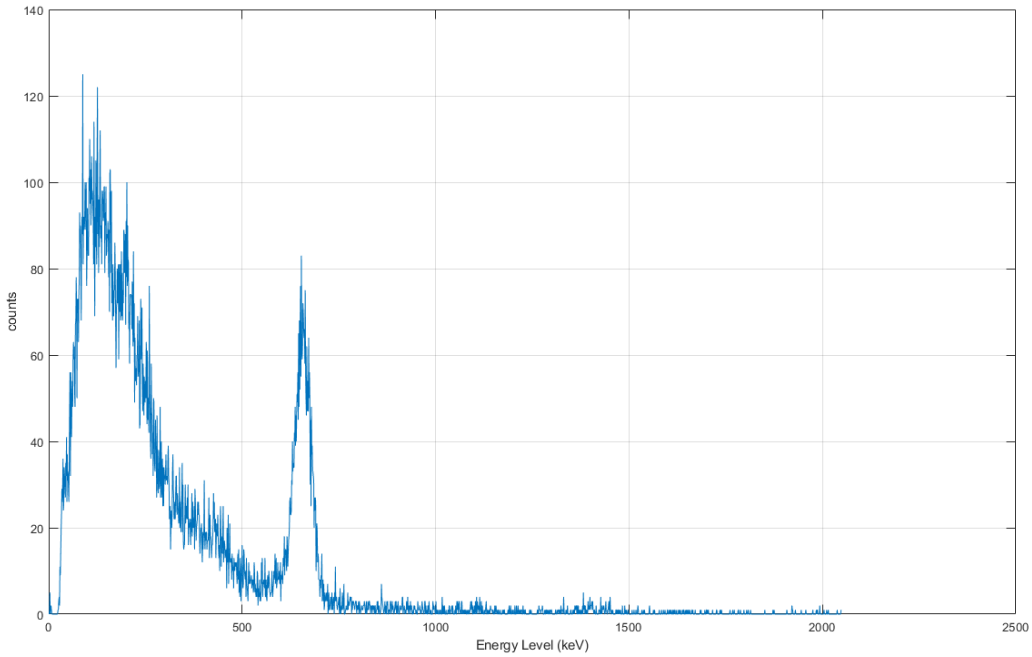

Figure 3.3: Cs-137 Gamma Spectrum

The energy peak in this gamma spectrum aligns directly with the gamma ray energy associ-

ated with ^{137}Cs (661.7 keV) shown in Figure 3.1. This provides an example of how isotopes may be identified by gamma spectroscopy, but ^{137}Cs is a relatively simple case. For isotopes with a more complex energy signature, additional techniques or software would need to be employed to enable accurate isotope identification. The large amount of energy located at the lower energy levels is largely due the background radiation present at the testing location.

Since the proposed mission plan involves flights conducted outdoors in various seasons of the year, the detectors used should be able to be operated in a wide range of temperatures. Generally, there is a temperature dependence that must be accounted for when operating in conditions other than room temperature. This correction is made by the software included with the USL detectors, and is reliable at temperatures from -40°C to 60°C. [1]

3.2 Radiation Detector Integration

This section contains all information pertaining to the selection, characterization, and implementation of the radiation detector and sources used for the bulk of research.

3.2.1 Detector Selection

The USL at Virginia Tech is fortunate to have access to a small selection of sodium iodide (NaI) detectors provided by Sandia National Laboratory for research projects. The two detectors available for use in this work are shown in Figure 3.4 and Table 3.1 shows the relevant details for each detector. Mass is of particular importance for this project as total payload weight significantly affects flight duration due to battery constraints and aircraft selection.

It is worth noting that both systems are able to be used with the same model of Multichannel

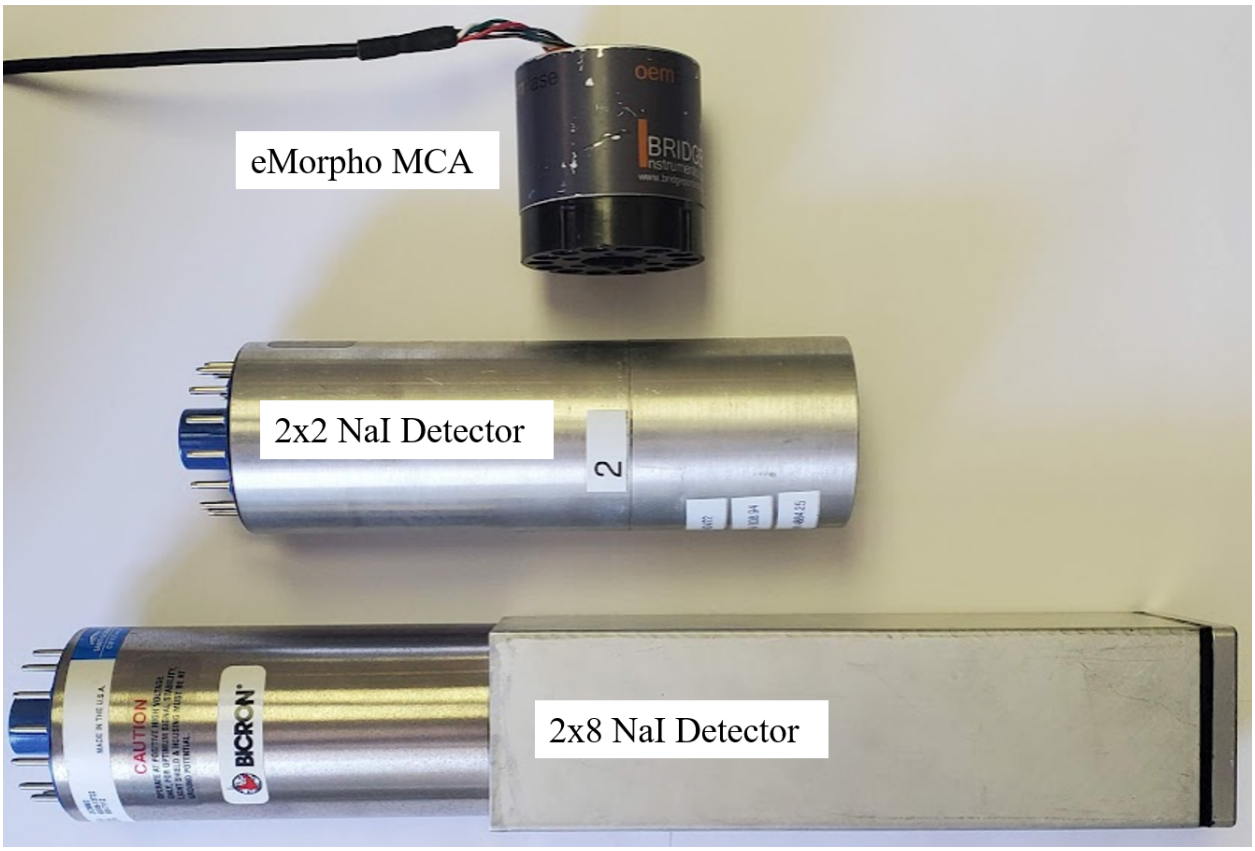

Figure 3.4: USL Detectors

Analyzer (MCA), labeled in Figure 3.4 as the eMorpho. This has the benefit of allowing both sensors to operate using the same software and testing scripts. The eMorpho MCA (produced by Bridgeport Instruments Inc.) interfaces via USB with the onboard companion computer. Testing scripts and custom software to interface with the companion computer were developed to streamline data collection and standardize testing.

In addition to the weight of the systems, the other main consideration for detector selection is the relative performance of the detectors. The UAS has the capacity to carry either detector at the expense of flight time, so it is necessary to determine if the smaller sensor performs sufficiently or if the larger sensor is needed. Therefore, a test plan was developed to determine the relative performance of each detector as shown in Table 3.2:

Table 3.1: USL Detector Details

Detector	Volume (cm^3)	Weight (g)	Resolution (%)	MCA Interface
2"x2" NaI (Alpha Spectra)	103cc	675g	<7.5%	eMorpho (Bridgeport Instruments)
2"x8" NaI (Saint-Gobain Crystals)	412cc	2510g	<7.5%	eMorpho (Bridgeport Instruments)

Table 3.2: Detector Selection Tests

Characteristic	Test
Directionality of sensor	Radial Testing at varying detector angle
Distribution of recorded counts	Long period collections (source and background)
Performance at varying distances	Collection at varying distances from source
Detecting counts from source vs. background	Comparing background only to source present

Directionality

Several tests were conducted with each sensor to determine the response of the detector as a function of detector angle to source. One-minute dwell time measurements at angles of 0, 45, 90, 135, and 180 degrees were recorded at distances of 1, 3, and 5 meters from the source. The counts were then divided by time to provide counts per second (cps). The source and detector were both elevated above the ground and in-plane. These tests were conducted outside of the USL in order to determine the performance of each detector in the same environment as the final system will perform (outdoor and above pavement). Figure 3.5 shows the setup for this test, which utilized the 41 μCi (40 μCi of ^{137}Cs and 1 μCi of ^{60}Co) available to the USL (discussed in 3.2.2 Radioactive Sources).

The purpose behind this test was to determine the detector response at different angles. This is important for several reasons. First, if one of the detectors exhibited a strong directional dependence it could potentially be used to more accurately locate a source. Second, strong directionality could lead to erroneous data if not properly accounted for when conducting localization. Figure 3.6 shows the results of this testing.

Figure 3.5: Experimental setup for directionality testing

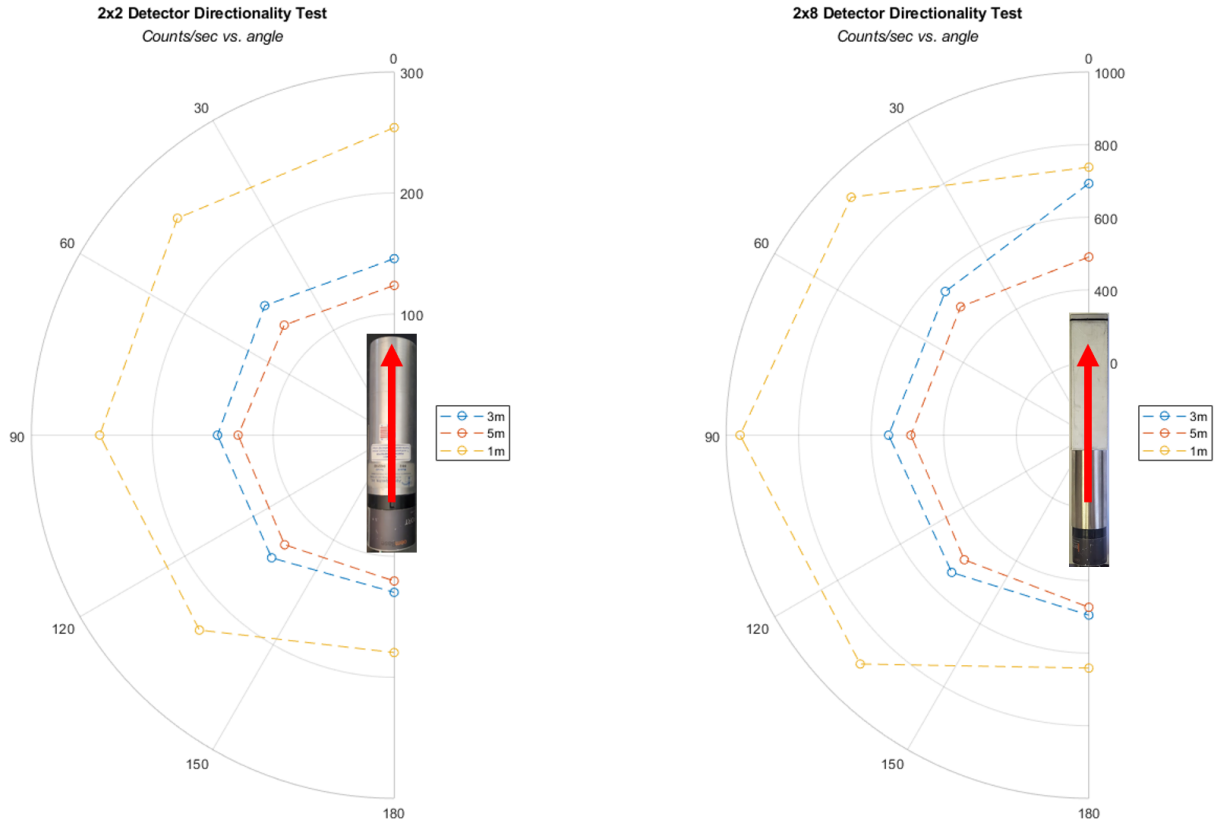

Figure 3.6: Directionality Test Results

The 2”x2” detector showed very little dependence on direction with most of the readings being very near 250 cps. The exception to this is towards the rear of the detector where the MCA is attached that saw a 28% reduction to 179 cps. This was expected due to the shielding and interference caused by the physical device located at this point. This amount of directionality does not influence the readings in a significant way due to the orientation of the detector mount used when attached to the UAS.

In contrast, the 2”x8” detector recorded much higher counts in some directions. Specifically, it showed a significant increase in counts in the range of 45°-135°. This would lead to higher counts being recorded when the source is to the side of the aircraft rather than in front or behind. This amount of directionality will not help with localization due to the symmetrical nature of these differences.

Significant shielding would be required for both detectors to achieve useful levels of directionality. Brewer suggests such a configuration shown in Figure 3.7. This would provide directionality to the extent that is needed to become beneficial for localization. To implement such a system, independent detectors should be isolated by implementing shielding material layers between each sensor (typically tungsten or lead). This alteration would provide information relating to the direction of the source in the relative ratios of counts seen at each isolated sensor.

Alternatively, the system could use a detector long enough such that the directionality is more exaggerated than that of the 2”x8” NaI sensor used in this testing. While this would provide a more definitive indicator for direction of source when compared to the small sensors used in this testing, the inherent symmetry of a rectangular crystal would lead to ambiguity as to which side of the long detector the source is actually located when a large reading is observed. This issue could be mitigated by implementing shielding to narrow the field-of-view of the sensor, but this would add additional weight to the system as well as reduce its

overall ability to sense gamma radiation.

This relative counting data (whether from a shielded sensor array or a single long detector with adequate directionality) could then be combined with information on the aircraft's heading to provide a real-time prediction of source direction in addition to proximity. This added level of information would be extremely useful in developing a system that autonomously plans its own flight path based on prior information, such as what Towler developed at the USL [16].

Unfortunately, this type of system would become prohibitively heavy for use on a small UAS (sUAS) such as the one used in this study. Because of this, directionality is not taken into consideration in the following sections. This makes the 2"x2" detector marginally better than the 2"x8" detector in this regard due to its lower dependence on direction, but neither sensor would prove unusable for this testing.

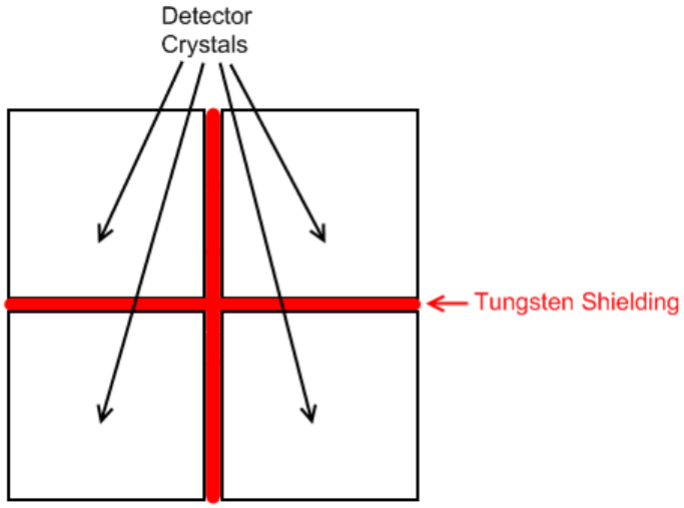

Figure 3.7: Directional Detector Configuration

Figure courtesy of Eric Brewer and Virginia Tech [7].

Distribution of recorded counts

For this project it was desired to conduct flights while collecting radiation data over a large area. To do this, the UAS would need to move constantly at a given speed (1 meter-per-second) while the radiation detector records data as to avoid battery loss due to stationary hovering. Since the system would be always moving, short dwell times for the radiation measurements are required as to not spread the measurement over too great an area. A dwell time of 1 second was selected for initial testing in order to avoid having to derive counting rate and thus introducing additional uncertainty. This is a very short collection period and results in significant statistical fluctuations when compared to longer dwell times. It was hypothesized that these statistical fluctuations would fit a Gaussian distribution and would not prove to be so large as to make localization impossible.

To determine if this dwell time would be sufficient for this purpose, an experiment was conducted to test the distribution of counts recorded by the detector in one second periods. Both detectors were programmed to record multiple one second measurements in a row. The detectors were set up to use a lossless mode to prevent the rapid collections from affecting the data.

The experiment was conducted outside to replicate the environment that the system would be performing in. Two tests were conducted with each detector:

1. 600 one second samples (10-minutes total) of background radiation
2. 600 one second samples (10-minutes total) of background radiation + source radiation

The results were then plotted for both scenarios using histograms while also overlaying a Gaussian curve using the experimental mean and variance of each data set. Figure 3.8 shows these results for both the 2”x2” and 2”x8” detectors. From this visualization it appears that the data for all scenarios is normally distributed. To further verify this, the MATLAB

built-in function for the Lilliefors test for normality was employed [13]. For all sets of data presented, the Lilliefors test confirmed normality. This adds quantitative confirmation of the conclusions of the qualitative analysis of the data performed in Figure 3.8.

It is worth noting that this data could also come from a Poisson Distribution. For the purposes of this section and paper, these two distributions are identical in their application due a relatively large mean value which allows for simplification to a Gaussian Distribution. The purpose in identifying the underlying distributions is to confirm that the uncertainty in the measured values matches what is expected [11]. Since the distributions match those expected from radiation detection, the following equation can be employed to determine measurement uncertainty for any given measurement:

$$\sigma = \sqrt{s^2} = \sqrt{\bar{x}} = \sqrt{x} \tag{3.2}$$

where σ is the error in a single measurement x, s is the variance, and $\bar{x}$ is the mean of the data set (which in the case of a single measurement is just x).

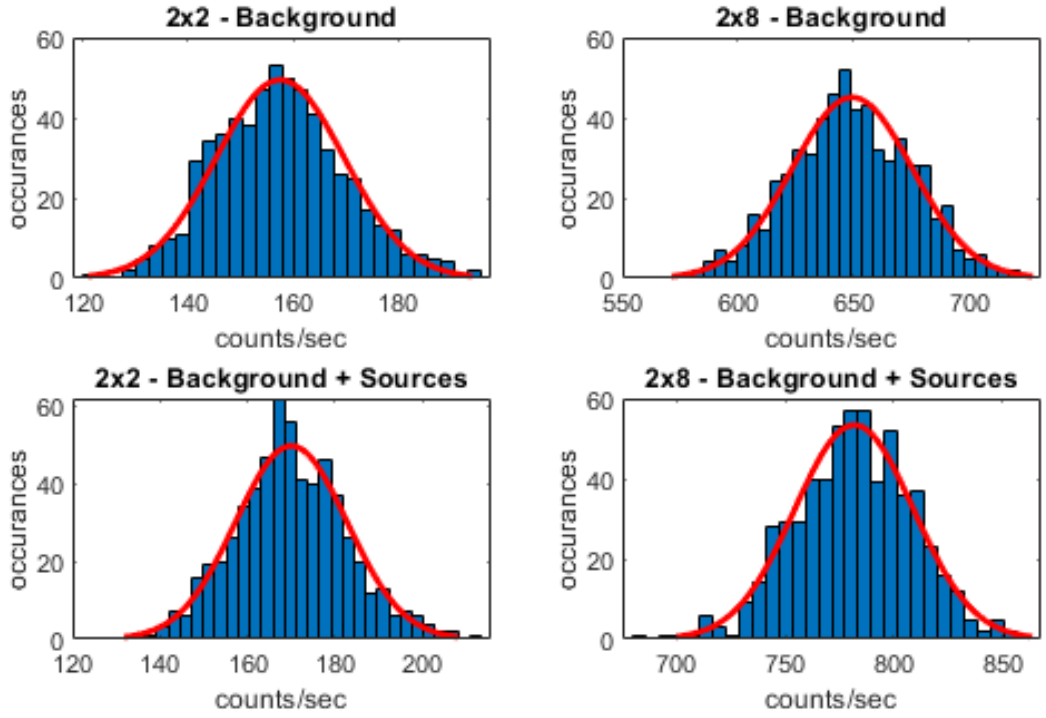

Figure 3.8: Histograms showing results of counting experiments with both 2x2 and 2x8 detectors. Gaussian (normal) distribution curve shown in red for each data set

3.2.2 Radioactive Sources

The USL has done extensive previous work regarding radioactive source localization over the past decade. Most of this work was done using a simulated source approximated with a inverse-square relationship between source strength and distance. Brewer discusses this in detail and the relevant equation is shown here [7]:

$$DetectedStrength = (\frac{1}{R^2}) * (SourceStrength) \tag{3.3}$$

where R is distance from detector to source. While this relationship provides a sound approximation of the behavior of radioactive materials, there are several drawbacks to this simplified

approach. First, this method assumes perfect performance by the detection systems with no statistical fluctuations in measurements. Second, this approach does not account for the addition of noisy background radiation that will pollute the data when testing with real detectors and sources. Therefore, for this project it was desired to test with real sources and detectors in outdoor environments.

Working with the Radiation Safety Office at Virginia Tech, a small quantity of radioactive sources were acquired to use for testing. Table 3.3 and Figure 3.9 show all sources used. All of these sources are low activity sources that fall under the exempt quantity rules set forth by the Nuclear Regulatory Commission [2] and do not require special licensing, but the activity is high enough to use for the purposes of this project. ^{137}Cs was selected due to the higher activity being exempt from licensing, and ^{60}Co was chosen to provide an alternate isotope to test the functionality of the detectors as well as demonstrate the gamma spectroscopy capabilities. Additionally, the ^{60}Co produces higher energy gamma rays at a higher rate than the ^{137}Cs. This allowed the ^{60}Co to be useful for testing despite its lower quantity.

Table 3.3: List of sources

Isotope	Activity
Cs-137	10 µCi (Quantity: 4)
Co-60	1 µCi (Quantity: 1)

It should be noted that these are not calibrated sources. Due to this, precise calibration of the detector count readings was not possible. However, the gain and voltage were able to be adjusted to provide accurate gamma spectra information using the gamma energy characteristics of the ^{137}Cs. This gamma spectrum calibration was confirmed by using the ^{60}Co source. In addition, these detectors were calibrated before being given to the USL and all experiments indicate that they are functioning properly.

The half-lives of each isotope are shown in Figure 3.9. All flight testing done for this thesis

was conducted on May 2, 2022. ^{137}Cs has a 30.08 year half life and therefore the reduction in activity due to time is negligible. The ^{60}Co has a shorter 5.27 year half-life and only around 92% the 1 μCi remained at the time of testing.

Figure 3.9: Sources

Final Detector Selection

From the testing conducted with the two detectors it was determined that the 2"x2" NaI detector would be used for the remainder of testing done in this project. The main reasoning for this is largely a practical consideration: the size and weight of the smaller detector would allow for testing with either Skyrad platform as well as longer testing sessions (as seen in Table 4.1).

In addition to the flight considerations, the omnidirectional qualities of the smaller detector are beneficial since directionality is not taken into consideration in this work. By limiting the effects of detector orientation, flight planning is simplified and aircraft heading is eliminated as an additional variable that would be present if the 2"x8" detector were used.

Chapter 4

Experimental Methodology

4.1 UAS Platforms and System Architecture

4.1.1 UAS Platforms

The UAS platforms used for the testing and experimentation were developed by a team at the USL. They are multi-rotor vehicles that were built to serve as a modular platform for several different projects and payloads. Two UAS's were used in this testing: the Skyrad X4 and Skyrad X8. These are shown in Figure 4.1. Both of these aircraft were designed and produced as part of a larger USL project relating to radiation detection and mapping.

Both systems operate using the same avionic systems, flight controller, and onboard computer. This makes it very simple to swap hardware and payloads between the two aircraft. The only significant difference between the two platforms is the propulsion system. The Skyrad X4 uses a traditional quad-copter configuration with four motors while the Skyrad X8 uses a coaxial motor configuration that includes eight motors.

This gives the X8 two advantages over the X4: it can support a heavier payload and it has propulsion redundancy in the event of a motor or propeller failure. This redundancy is particularly critical when flying over people and property. The major advantage of the X4 is flight endurance. Since it uses the same battery and half of the amount of motors it is able

to fly for a much longer time than its X8 counterpart (shown in Table 4.1).

(a) Skyrad X4

(b) Skyrad X8

Figure 4.1: UAS Platforms

Table 4.1: Skyrad Platform Endurance Limits and Payload Capacities

Aircraft	2"x2" (675g)	2"x8" (2510g)
Skyrad X4	51.4 minutes	Over Limit
Skyrad X8	36.8 minutes	27.2 minutes

Due to proven superior reliability, the Skyrad X8 was chosen for all testing. There is also the benefit of the propulsion redundancy which greatly reduces any risk associated with test flights.

4.1.2 System Architecture

Hardware

The hardware used for this testing is shown in Figure 4.2. Of particular importance is the Jetson Xavier NX , the onboard computer installed on the UAS (referred to as the ”Xavier”). This computer is capable of running all software needed for the radiation detector as well as performing some of the data analysis during and after flights. This enables scans to be conducted with live updates and scan information displayed to the pilot via the ground

control station. This will be particularly useful for detection and monitoring in the field applications for which this system is eventually intended.

The Xavier communicates with the Ardupilot Cube Orange to supplement the radiation collection data with the altitude, latitude, and longitude of the aircraft at each point that radiation data is collected. The ground station enables the user to create missions by selecting a polygon search area on a satellite image of the site being investigated and then uploads that mission to the Cube Orange to be stored upon the aircraft. Finally, the GNSS (commonly GPS) provides the system with its position and compass heading.

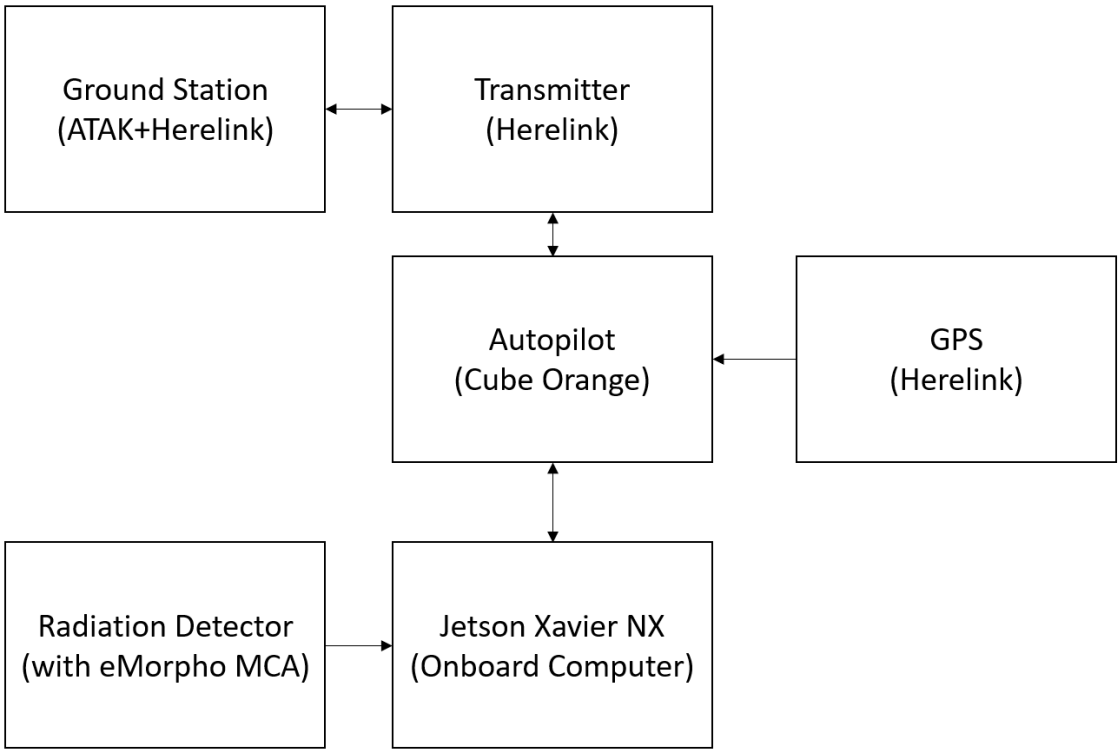

Figure 4.2: Hardware System Design

Software

There are two main software packages that are were developed for this project: flight planning/mission creation, and post-flight data analysis. This thesis focuses on the post-flight data analysis which could be conducted using the Xavier onboard computer. For this research, a laptop computer was used to allow for easier development of analysis programs and for the increased processing power. In addition to these benefits, using the laptop computer for mapping and analysis allows for multiple algorithms and techniques to be tested and compared to one another relatively quickly and easily. Figure 4.3 shows the software located on each piece of main hardware.

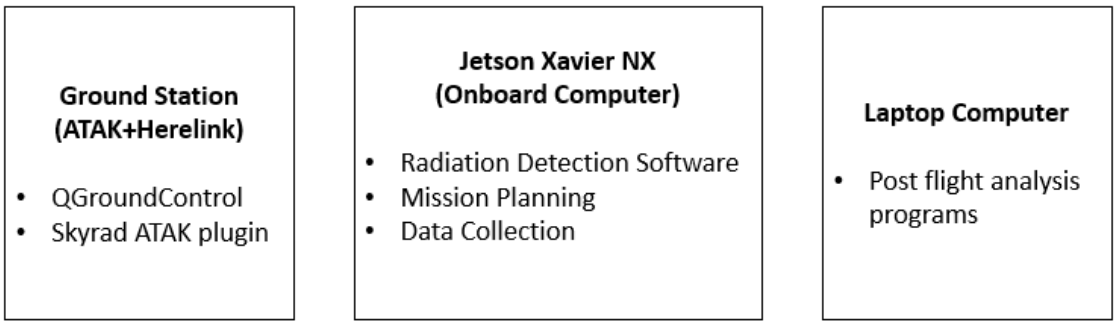

Figure 4.3: System Software

Of particular interest is the use of both the Xavier and laptop computers for data management. Through ROS, mavROS, and the radiation detection software it was possible to develop a program that combines all of the IMU (Inertial Measurement Unit), GPS, and radiation data into simple JSON files. These files contain all of the radiation scan data from a flight (GPS data, radiation counts, and radiation spectral data) and allow for easy transfer from Xavier to Laptop for processing and viewing. The software was developed to allow for easy parsing and loading of the data into Matlab as well, as Matlab is the main application used for the data post processing and mapping.

Future work includes transitioning all programs and software currently on the laptop com-

puter to the Xavier onboard computer. Not only would this streamline flight operations, it would allow for the development of in-flight mission updates and intelligent flight planning based off of real-time results. This work assumes a static flight plan, but through machine learning and further testing, a method of producing dynamic flight plans could be developed and lead to more efficient missions and search strategies. This would, among other tasks, require developing Python equivalent software for the processes currently conducted using MATLAB. Once these things are done, this system would be entirely self contained and would prove very capable as a system to be used in the radiation monitoring industry.

4.2 Experimental Setup

This section contains information regarding the experimental setup and relevant equipment used for data collection.

4.2.1 Test Location

Preliminary testing of flight systems, radiation detection software, and data collection was conducted in the backyard test ground of the USL. This proved to be useful due to the nature of the work required to prepare the UAS for large scale testing. Specifically, integrating the custom radiation collection software written for this work with the aircraft autopilot and flight controls required many short tests to troubleshoot issues as they arose.

All main flights were conducted at the Kentland Experimental Aerial Systems (KEAS) Lab at Virginia Tech. Specifically, all flights were conducted over the runway located outside of the main lab building. The runway was chosen as the test ground instead of a grass field or gravel lot for several reasons. First, the flat nature of the runway will eliminate any

effects due to uneven terrain (aircraft altitude fluctuations, ground effects on background radiation). Second, the runway works very well with the downwards facing LiDAR module installed on the UAS to ensure accurate altitude measurements and control. Finally, the asphalt runway aligns with the eventual application of the project which will be scanning parking lots filled with vehicles or equipment.

4.2.2 Source Placement

The sources were placed on top of a tripod in order to elevate them above ground level. This increase in overall height reduces the risk associated with the flights (higher flight altitude reduces the impact of altitude fluctuations) as well as better simulates the geometry of a real world scanning scenario. The sources were placed at a height of 1.5m above the ground with no shielding present. They were arranged in plane with one another and attached to the tripod to prevent the rotor downwash from displacing the relatively small and lightweight sources. This setup of the radioactive sources can be seen in Figure 4.5.

Since the size and arrangement of the sources were very small in relation to the search path the sources were considered to be a single point source. This assumption was made with the consideration that the distance between the individual sources (d in Figure 4.4, distances of 1 cm) were much smaller than the distance between the sources and the aircraft/detector (D in Figure 4.4, distances over 1.5m). The distance between detector and source (D) would be constantly changing with each scan as the UAS changes locations, but the minimum value for D would always be the scan altitude (minus the 1.5m tripod height).

In a real world scenario, shielding could be present in order to further hide the radioactive material from detection. In this testing there was no shielding added, but instead the tests were flown at greater and greater distances from the sources to simulate the lower radiation

signal coming from a shielded source. Nothing regarding shielding and source concealment can be learned from this testing, only the ability of this system to detect equivalent levels of activity from shielded or unshielded sources. If one were interested in applying this study to shielded sources, the activity level located at the outside edge of the shielded source would need to be determined (either analytically with the knowledge of source and shielding [11] or by experimentation).

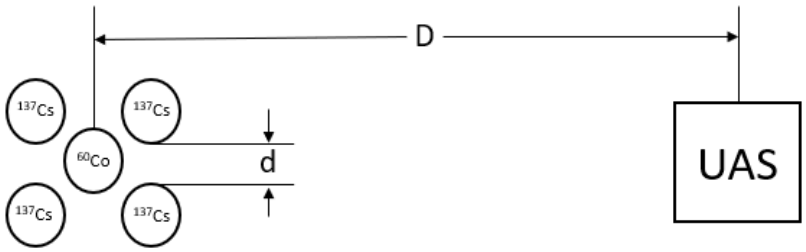

Figure 4.4: Experimental Setup - Source G eometry

Figure 4.5: Experimental Setup - Aircraft and Location

Chapter 5

Testing and Results

5.1 Testing

Throughout the development and testing of the Skyrad system there have been dozens of flights and radiation scans conducted. For the purposes of this work, three flights were conducted once the system was fine tuned and functioning well. All of these flights were flown in quick succession to minimize any changes in the environment, and Table 5.1 details the specific flight parameters chosen for each flight. The variable being tested is the AGL (above ground level) altitude. All flights were flown at relatively slow speeds compared to earlier testing in order to provide a very dense grid of data.

Altitude	Aircraft Speed	Collection Dwell	Source?
3m AGL	1 m/s	1 second	Yes
5m AGL	1 m/s	1 second	Yes
7m AGL	1 m/s	1 second	Yes
3m AGL (Control)	1 m/s	1 second	No

Table 5.1: Specific flight parameters for tests

By choosing 1 m/s as the flight speed for all tests, points can be removed to simulate faster speeds. For example, with every other point removed (i.e. 1, 3, 5, etc.) this data would simulate an aircraft speed of 2 m/s. This will later be used to examine the effects of grid density on the efficacy of the system.

All tests were conducted with the same mission plan and way-point files to ensure consistent

search area size. An area approximately 20m wide by 30m long was selected to provide an overall search area of approximately 600m^2. Only the altitude of the UAS was altered between tests.

In addition to these tests, measurements of the background radiation levels were taken immediately prior to each main scan at the same altitude as the scan in order to minimize effects of time and altitude on the background levels compared to the scan levels. Finally, a control scan was performed at 3m with no source present in order to provide a baseline set of data to compare the main scans to.

Finally, a nadir image was taken of the runway and used for mapping overlay to assist in visualization. It is worth noting that all location data is referenced only to the aircraft GPS. This reduces error due to differences between satellite imagery and UAS GPS data. In addition, GPS drift on the UAS was minimized by limiting the amount of time between flights and confirming source location for each test.

5.1.1 Identical Flight Path Used for All Tests

A flight was planned using the Herelink GCS (ground control station) for an initial flight to verify system functionality prior to main test flights. The flight path for this mission is shown in Figure 5.1 in blue. The source location is shown as the black triangle (which has a leg length of approximately two meters, for scale).

All subsequent flight testing used the same way-point mission and flight plan from the initial flight to ensure consistency between runs of different altitudes. It is worth noting that the flight path does not precisely align with the paved runway. This offset is due to the use of satellite imagery for flight planning. The image shown, flight path, and source location plotted are all in reference to the aircraft GPS and are accurate with regard to one another.

Figure 5.1: Flight path plotted over aerial image with source location

5.1.2 Radiation Count Levels Directly From Detector

The first analysis conducted on the data from the flights was simply to plot the results onto a nadir image of the KEAS runway taken prior to testing. Figure 5.2 shows a grid of these results with the relevant mission speeds and altitudes labeled above the maps.

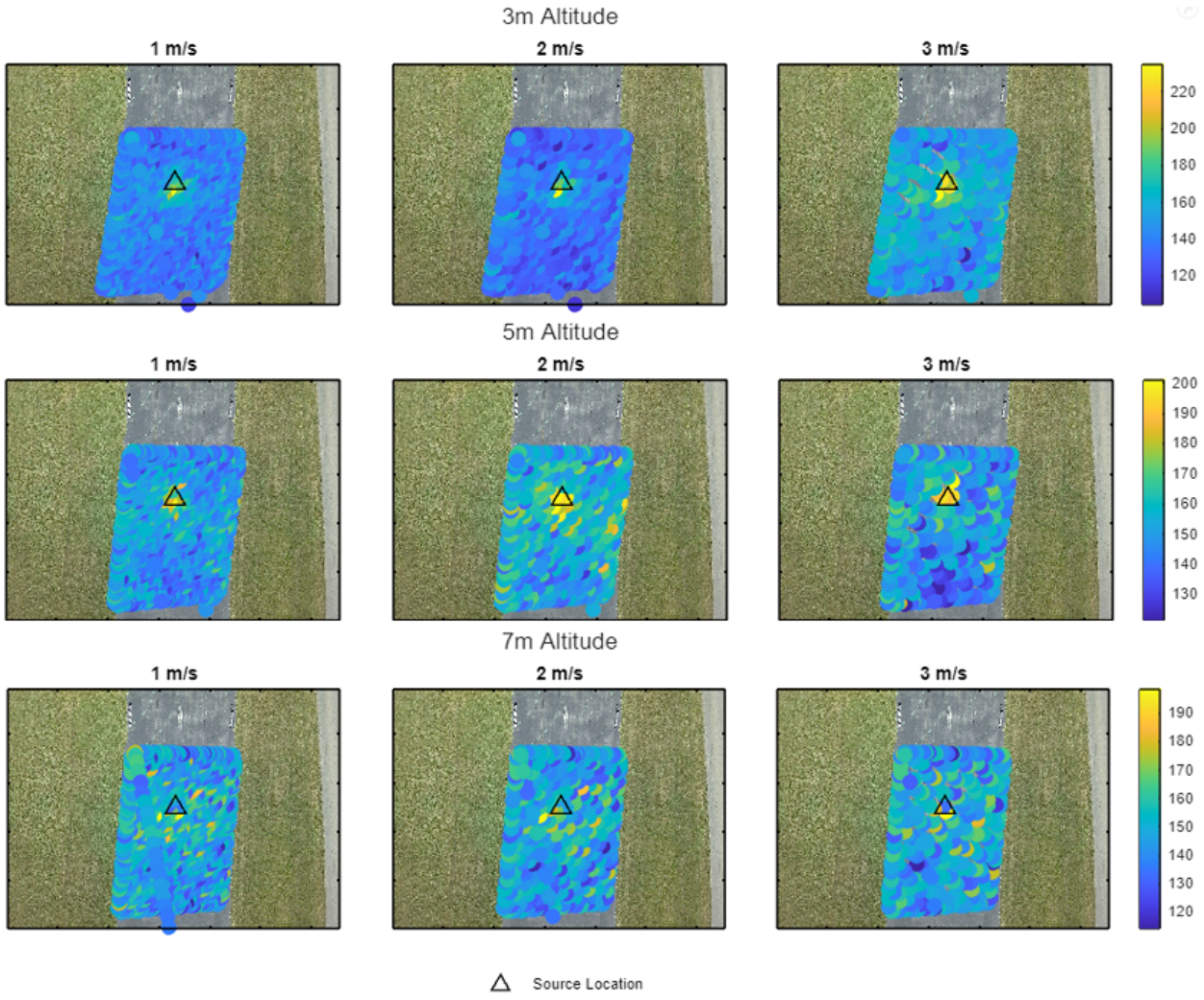

Figure 5.2: Unprocessed counts at varied speeds and altitudes

The results seen in Figure 5.2 were very consistent with what the team saw throughout development of this system. At low speeds and low altitudes, these raw data points can be used to qualitatively determine an estimate of the source location within roughly 2m.

While this is useful, it was desired to have a better way of demonstrating source location and detection probability. Figure 5.3 shows a similar set of plots, but this time with the average background radiation level subtracted from the detected counts.

5.1.3 Background Subtracted Values

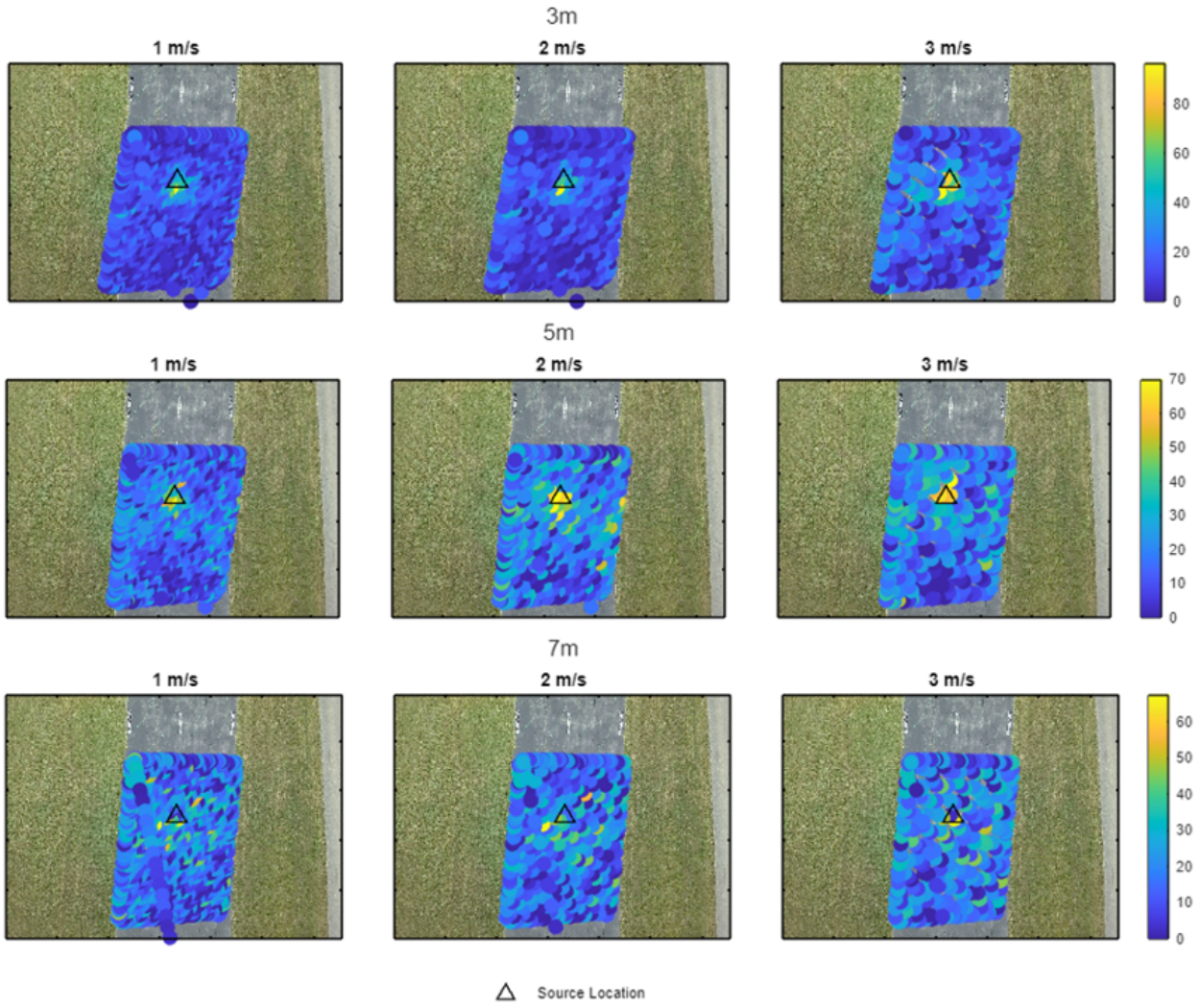

Figure 5.3: Background subtracted counts at varied speeds and altitudes

By subtracting the background radiation it becomes easier to determine the location of the potential source. Due to the statistical nature of the detector discussed in section 3.2.1, many of the values return as negative (particularly for data points located far from source). To aid visualization, Figure 5.3 shows any negative values as 0.

5.1.4 Background Subtracted Values with Alarm Levels

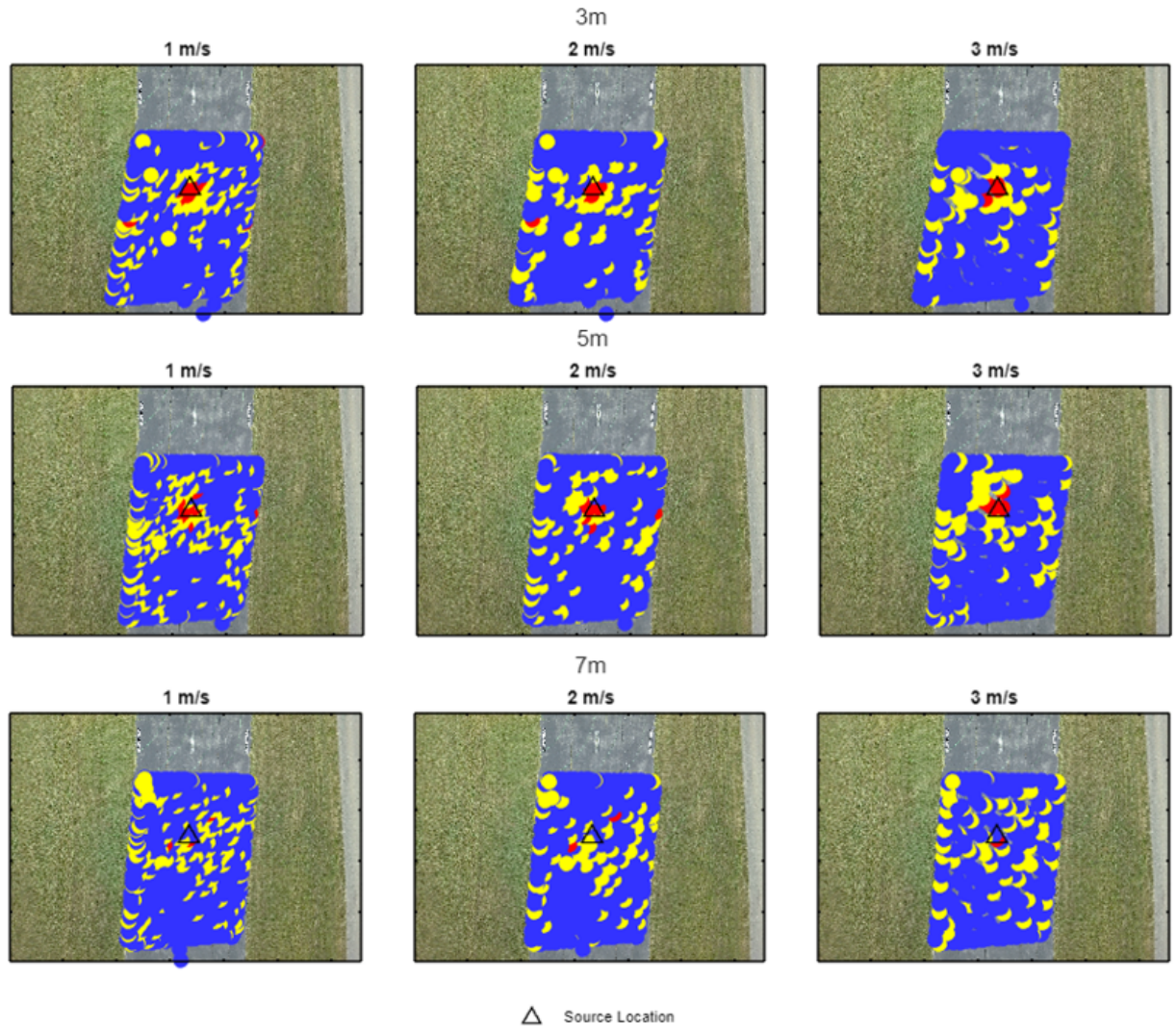

Figure 5.4: 3 alarm levels at varied speeds and altitudes

To further provide confirmation for detection, scripts were developed to produce 2 "alarm levels" based off of definitions of minimum detectable activity first introduced by Currie [10] and described in the Knoll text [11]. When a false alarm rate of 0.05 is specified, a critical level (or alarm level, L_C) can be calculated using Equation 5.1.

$$L_C = 2.33\sqrt{N_B} \tag{5.1}$$

N_B is the level of background activity measured prior to sources being introduced. This establishes the lower bound for measurements that can ensure a false-positive rate of <5%. In Figure 5.4 measurements that fall below this value are shown in blue.

In addition to this critical level, Currie defined the minimum number of counts needed to ensure a false-negative rate of <5%. This value, N_D, is used in this context to highlight the measurements taken that have a very high likelihood of being caused by a nearby source. This value is calculated using the "Currie equation" [10]:

$$N_D = 4.65\sqrt{N_B} + 2.71 \tag{5.2}$$

which provides N_D, the minimum value of measured counts that corresponds to a 95% probability that a source is present. Values above this threshold are shown in red and values that fall in-between L_C and N_D are shown as yellow in Figure 5.4. The information introduced in this section is also used in subsection 5.2.1 to provide the levels used to determine detection ability for alternative sources besides the ones used in flight testing in this section.

5.1.5 2-D Surface Fitting

The final method used in this project to create a contour map of radiation location probabilities was to implement a simple 2-D surface fit over the data. During the testing and demonstrations with radiation detection officers from CBP (Customs and Border Protection), this method proved to be the most intuitive and attractive option for communicating

the results of a scan.

This surface fit was applied to both the raw counts as well as the background subtracted values. Figure 5.5 and Figure 5.6 show these results respectively (note that slight plotting artifacts are present due to the surface fitting methods used). This is a similar approach as that taken by Towler in his work [16], but with a pre-programmed flight path rather than contour following algorithms.

The simplified approach shown in this work is effective when mission requirements mandate the searching of a large area rather than the rapid location of a known source. This more relaxed mission structure is directly relevant to the field of detection and deterrence since large areas of cargo and vehicles must be searched regardless of whether or not a source is present.

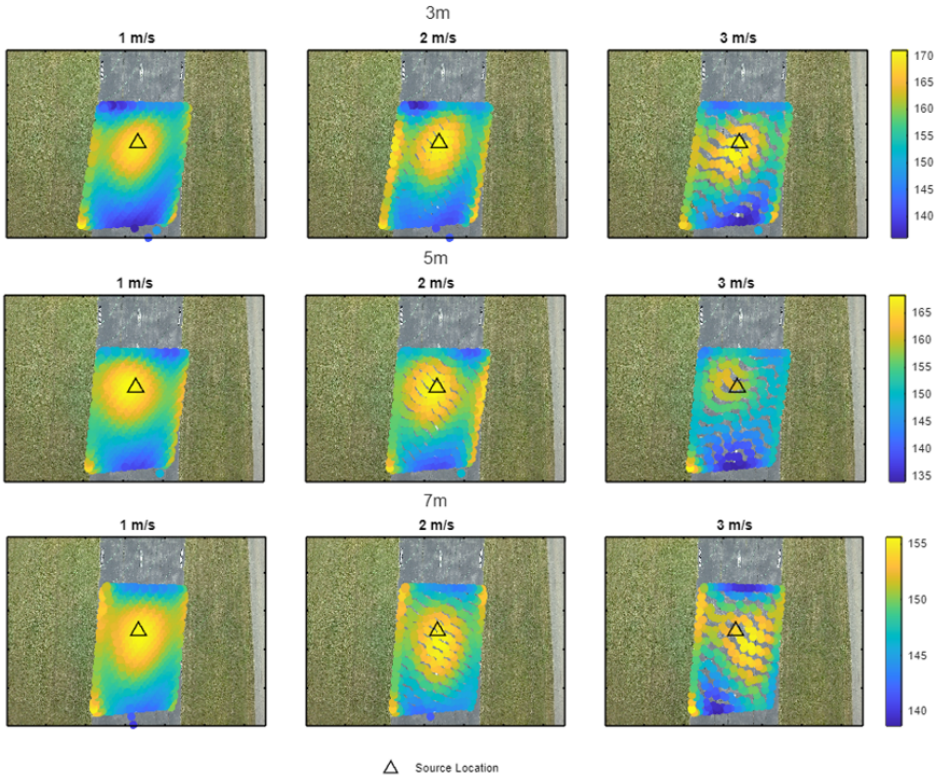

Figure 5.5: Contour plot of counts at varied speeds and altitudes

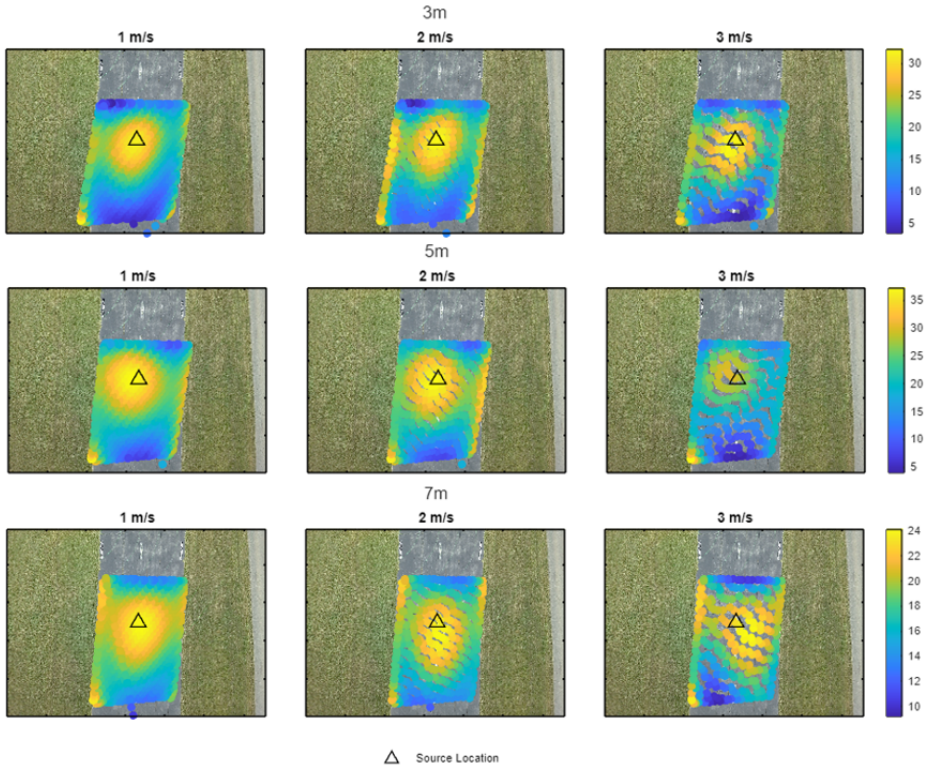

Figure 5.6: Contour plot of background subtracted counts at varied speeds and altitudes

5.2 Savannah River National Laboratory Isotope Testing

To supplement the data from the smaller sources available to the USL for flight testing, a trip to Savannah River National Laboratory (SRNL) was conducted to collect data using the USL NaI detectors. This was done to both quantify the ability of the detectors to sense sources other than ^{137}Cs and ^{60}Co and to collect information on the energy spectrum to determine if source identification would be possible using the UAS mounted detector system.

A variety of sources were able to be studied at the SRNL Calibration Lab. Table 5.2 shows these sources that were examined. Of particular note are some of the more controlled and

regulated isotopes, such as ^{235}U and ^{239}Pu.

Table 5.2: Sources tested at Savannah River National Laboratories

Source	Source Strength (μCi)
Pu-239	89,941.068
U-235	190.857
Eu-152	140.835
Ra-226	64.848
Cf-252	7.005
Co-60	176.535
Ba-133	96.211

Two tests were conducted with each source tested. First, a long dwell time was recorded at a relatively close range (3 minute dwell at a 2 meter distance). This measurement was taken to determine the ability of the detectors to perform gamma spectroscopy at a range achievable by the UAS. For the scope of this work, no gamma spectroscopy software/package was used to analyze this data. Instead, manual inspection of the energy peaks was used to determine a qualitative efficacy of the isotope identification ability of the system.

For the second round of testing, the detectors were programmed to record 1-second dwell time measurements in quick succession. This was done to best emulate the type of detection that the system is performing when the UAS is in flight and recording. The radioactive sources were then moved to different distances to simulate different flight altitudes. The distances for this testing were selected to be 2, 3, 4, 5, and 10 meters.

While real-time isotope identification at higher scanning speeds may prove infeasible, the results from the SRNL study show that these isotopes can be identified at the distances that the UAS is able to achieve. Therefore, this work recommends a two-stage flight plan when isotope identification is desired: a faster flight covering a large area to locate potential sources, and a second flight with extended dwell times hovering over the previously marked locations. This extended dwell would prove effective at distances up to 10m when used with the 2”x8” NaI detector depending on source strength, but lower altitudes would produce

more distinct gamma spectra as well as require less overall time to achieve the same result.

5.2.1 SRNL Detection Study

The main testing done at SRNL was to emulate a detection flight. Thirty 1-second samples were taken in the same way that the collections during UAS flight were recorded at a variety of distances. This data was then compiled into a series of frequency plots. These plots utilize the Currie limit definitions outlined in subsection 5.1.4 [10].

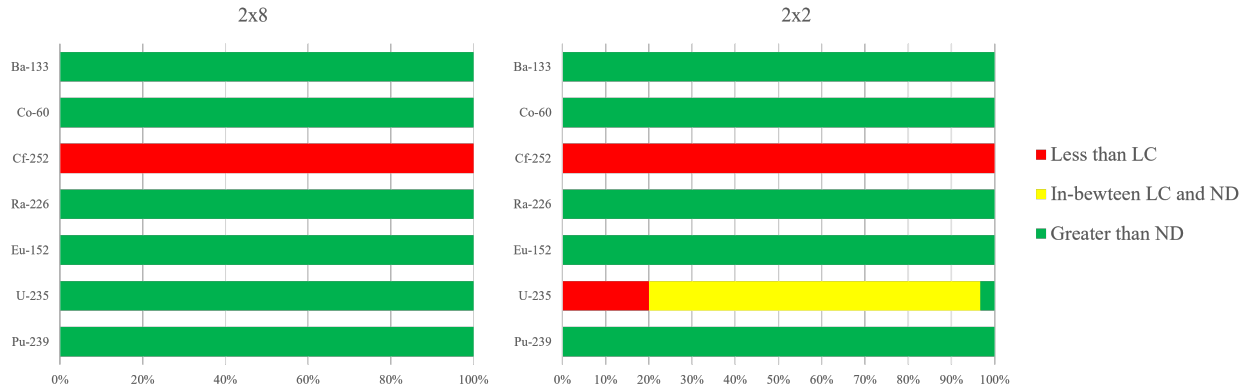

Figure 5.7: 2 meter results from SRNL testing showing detection probability

In these figures, the green area refers to the frequency of scanning results that fall above the N_D level which results in the probability of a source being present being higher than 95%. Red refers to results that fall below the L_C level which is determined based on a 5% false-positive rate. Yellow refers to values that fall in-between these two thresholds.

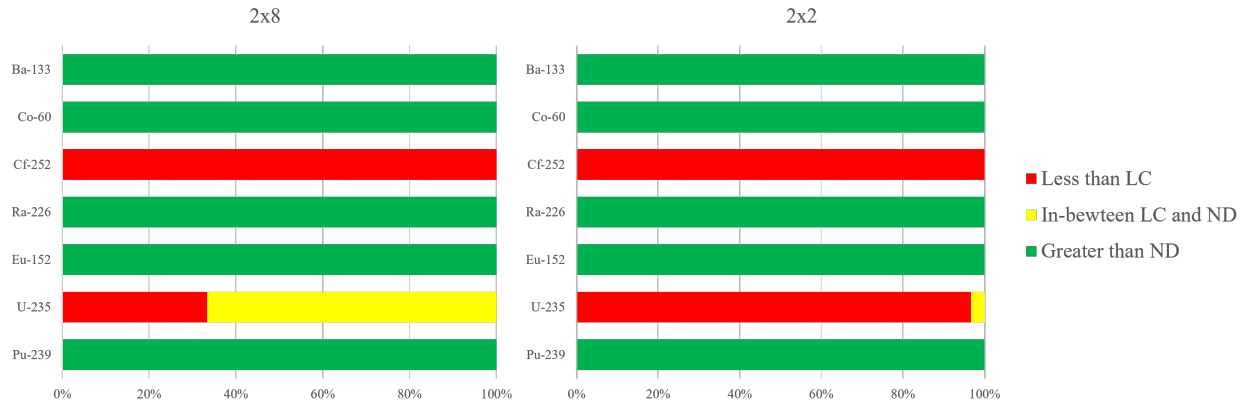

Figure 5.8: 3 meter results from SRNL testing showing detection probability

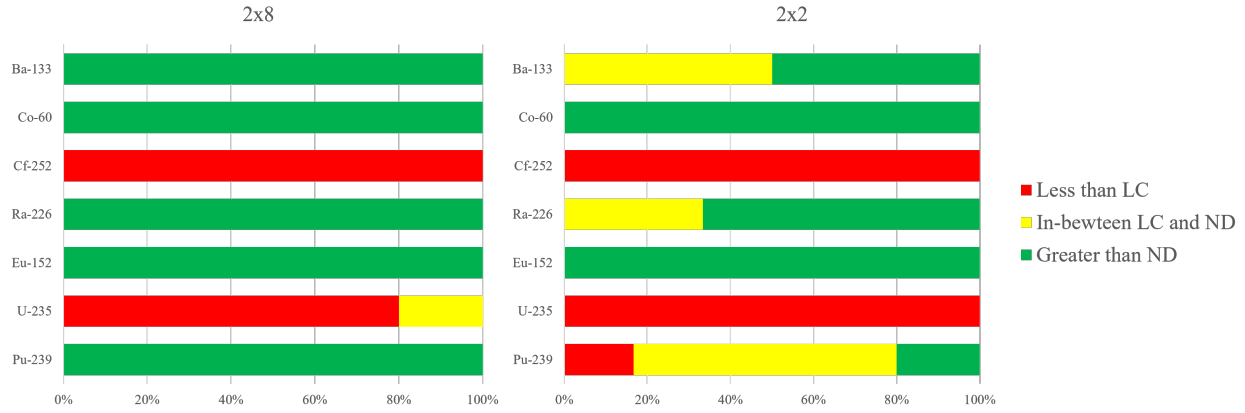

Figure 5.9: 4 meter results from SRNL testing showing detection probability

From these plots it becomes obvious that the larger 2"x8" detector is able to effectively operate at slightly longer ranges than the 2"x2" option. This benefit may be nullified depending on UAS performance and ability to fly at lower altitudes if the smaller detector is used. Mission parameters and requirements will drive the decision between detector sizes and these results show that either detector can successfully detect a variety of gamma-emitting sources.

Future systems and detectors can be compared to this data and existing detectors available to USL to predict detection performance for a variety of sources and source activities that

may prove difficult to test with otherwise.

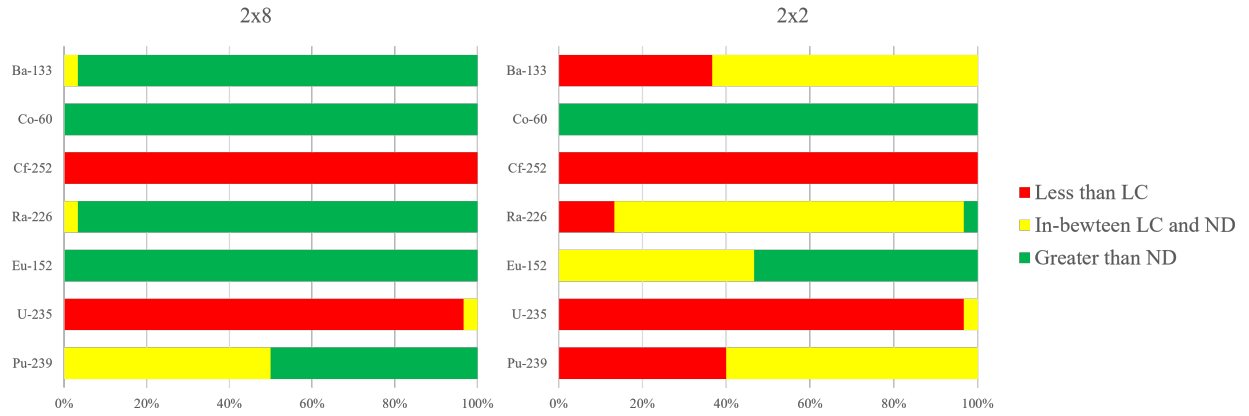

Figure 5.10: 5 meter results from SRNL testing showing detection probability

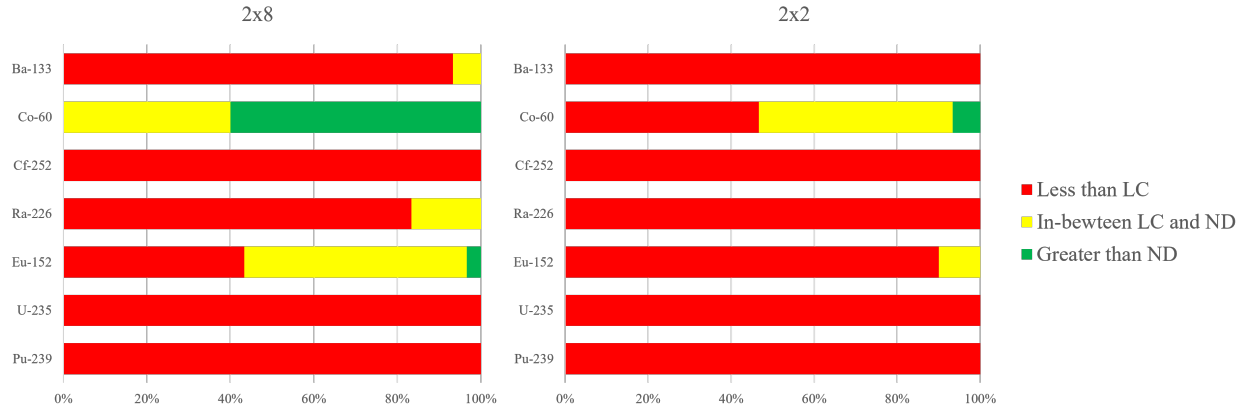

Figure 5.11: 10 meter results from SRNL testing showing detection probability

Obviously these results are very specific to the types of isotopes tested as well as their respective activity levels. Figure 5.11 shows that even at 10m the 2"x8" detector is able to sense a strong gamma-emitter such as Co-60. Additionally, many of the gamma rays detected in this study are due to daughter isotopes rather than the parent isotope being tested. This once again reinforces the need to incorporate intelligent isotope identification in future efforts.

In addition, the inability of either detector to sense ^{252}Cf (which is a much stronger neutron

emitter than gamma ray emitter) showcases the need for alternative detector technologies for different source types. Regardless, this information will prove valuable in optimizing future mission and UAS design decisions for sources other than ^{137}Cs and ^{60}Co which were the main focuses of this work.

5.3 Operational Considerations

The information outlined in the previous sections highlights the efficacy and potential impact the use of drones will have on the field of radiation detection and deterrence. Advancements in UAS technology will continue to expand the capabilities and impact of autonomous uncrewed radiation scanning, especially as better instrumentation and higher payload capacity aircraft are developed.

As UAS based detection systems are further adopted into this field, concepts of operations and standard practices must be developed to effectively implement autonomous scanning. This work recommends that UAS systems and mission planning be optimized for specific roles and tasks. Designing specialized systems and missions will ensure efficient, safe, and effective scanning in whatever end-use application is desired.

The data shown in section 5.1 illustrates the detection ability of relatively fast UAS flight. These quick "rough" scanning missions can then be repeated and refined to investigate potential source locations. As these systems further develop, the repeat missions can be integrated into the initial flight using real-time mission planning and updating.

After the relatively quicker scans to determine source presence, this work recommends a stationary dwell period be conducted over any assumed source locations. This longer dwell (on the order of a few minutes) would allow for high statistical certainty as it relates to

source presence. In addition, this longer dwell would allow for capable sensors to perform isotope identification to further increase the utility of remote scanning missions.

5.3.1 A Comparison to Existing Mobile Detection Technology

It is worth mentioning that this system was compared briefly with existing commercial radiation detection equipment. During on-site testing with Customs and Border Protection (CBP) officials, the RadSeeker system by Smiths Detection was compared with the UAS mounted detector system. Data offload from the RadSeeker system was not feasible, so only a qualitative comparison of the systems can be made.

Both systems performed almost identically when it came to detecting source strength and location. This is to be expected as both systems utilize a very similar NaI detector. The advantages of the commercially available system become obvious when employing the source identification capabilities. The RadSeeker was able to quickly output a prediction of the gamma-emitting radioisotope while the UAS mounted system requires a skilled operator to examine the gamma energy spectrum to determine the specific source being measured.

This shortcoming could be overcome by implementing one of the commercially available source identification software packages, but that was not done in the scope of this project. For the purposes of this work, it is sufficient to claim that the UAS mounted detection system has the potential to augment and enhance existing CBP operations in the field of radiation monitoring.

Chapter 6

Conclusion and Future Work

The main purpose of this project was to implement radiation detection onto a UAS platform and provide an analysis for the efficacy of this combination in real-world environments with real point-source nuclear material. This work specifically investigates low-altitude scanning via sUAS (small UAS). Advancements in this area will create a safer environment for workers in the detection and deterrence field as well as facilitate more robust responses to potential nuclear incidents. In addition to the increased safety for human operators, autonomous and remote radiation scanning will provide large cost savings and increased efficiency of the highly skilled operators required for this work.

This work also outlines the integration and characterization of a UAS mounted NaI scintillation detector. Significant effort was required to fully determine the capabilities of these detectors and to integrate them into a UAS system with fully autonomous flight and reporting. This research effort also includes the development of custom radiation detection software for use with the Skyrad system. Flight testing and tuning of this system and software was conducted and several radiation scanning missions were flown to validate and showcase the detection and mapping capabilities of the system.

The latter sections of this work focus on various techniques to display and process the data to become useful for localization and detection for eventual end-users and stakeholders. These techniques proved effective for qualitative determination of radioactive source location. In addition, experimental data was collected and analyzed to better inform future UAS designs

and mission planning in this field.

6.1 Future Work

This area of research has a long history within the USL as well as a bright future. The project which this work was a part of has continued on and successful missions have been conducted at the Port of Baltimore for Customs and Border Protection officials as well as for Coast Guard officials at Fort Macon in North Carolina. The applications for autonomous radiation detection are plentiful and demonstrate a need for commercial systems such as Skyrad.

To build on this work, additional sensor types should be investigated. The detectors that were used for this work were readily available to the USL and may not have been optimal choices if all commercial options had been considered. New developments in radiation detector technology that provide smaller, lighter, and higher resolution will transfer directly to improved detection via UAS. One particular. example of a detector technology that could be evaluated in future work is a LaBr type detector. In addition, alternative detectors could be studied (such as solid-state semiconductor based detectors) that provide the expanded ability to perform neutron detection and more thorough isotope identification. This ability would be highly valuable as several of the highly-regulated isotopes emit alpha and beta particles much more strongly than gamma rays.

Additionally, this work could be expanded on to include that of Towler and Brewer and implement Bayesian principles and prediction for real-time autonomous mission alterations and optimizations [16][7]. This would not necessarily improve the system performance in a scanning scenario in which a source may or may not be present, but could prove extremely valuable in a search scenario in which a known source is required to be found.

Another avenue for future work in this field would be to implement swarm technology (multiple UAS conducting a coordinated mission) to much more quickly scan large areas. Having multiple systems with dedicated roles would greatly increase the speed and accuracy of the mission. Ground based rovers could be integrated into this swarm that would carry much large detectors capable of sensing isotopes through shielding.

Ultimately, the continuation of this project should strive to further the development of UAS based radiation detection. As both fields (UAS and radiation detection) continue to improve, research and innovation will be required to effectively leverage the strengths and benefits that this unique combination of technologies provides.

Bibliography

[1] eMorpho data sheet, .

[2] NRC regulations - exempt quantities, . URL https://www.nrc.gov/reading-rm/doc-collections/cfr/part030/part030-0018.html.

[3] Nuclear smuggling detection and deterrence data analysis annual report FY2018, .

[4] J. S. Belrose. Reginald aubrey fessenden and the birth of wireless telephony. 44:38–47. doi: 10.1109/MAP.2002.1003633. URL https://ui.adsabs.harvard.edu/abs/2002IAPM...44...38B. ADS Bibcode: 2002IAPM...44...38B.

[5] Sean M Brennan, Arthur B Maccabe, Angela M Mielke, and David C Torney. Radiation detection with distributed sensor networks. 37(8):10.

[6] Allan Brettman. Drones fly low and slow for radiation detection. URL https://www.pnnl.gov/news-media/drones-fly-low-and-slow-radiation-detection.

[7] Eric T Brewer. Autonomous localization of 1/r2 sources using an aerial platform.

[8] Louis Brown. *Technical and Military Imperatives : A Radar History of World War 2*. CRC Press. ISBN 978-0-7503-0659-1. URL http://login.ezproxy.lib.vt.edu/login?url=https://search.ebscohost.com/login.aspx?direct=true&db=nlebk&AN=27525&scope=site.

[9] Amoret Bunn, Katie Wagner, Deborah Fagan, Harish Reddy Gadey, Tracy Ikenberry, Kameron Markham, and Moses Obiri. Drones for decommissioning. URL https://www.osti.gov/servlets/purl/1923755/.

[10] Lloyd A. Currie. Limits for qualitative detection and quantitative determination. application to radiochemistry. 40(3):586–593. doi: 10.1021/ac60259a007. URL https://doi.org/10.1021/ac60259a007. _eprint: https://doi.org/10.1021/ac60259a007.

[11] Glenn F. Knoll. *Radiation detection and measurement*. John Wiley, 4th ed edition. ISBN 978-0-470-13148-0. OCLC: ocn612350364.

[12] C. Michael (Charles Michael) Lederer, Jack M. Hollander, and Isadore Perlman. *Table of isotopes*. Wiley, 6th ed. edition. ISBN 0-471-52115-9 978-0-471-52115-0 0-471-52116-7 978-0-471-52116-7.

[13] Hubert W. Lilliefors. On the kolmogorov-smirnov test for normality with mean and variance unknown. 62(318):399–402. doi: 10.1080/01621459.1967.10482916. URL https://www.tandfonline.com/doi/abs/10.1080/01621459.1967.10482916. Publisher: Taylor & Francis _eprint: https://www.tandfonline.com/doi/pdf/10.1080/01621459.1967.10482916.

[14] Aleksandra Peeva. New drone technology for radiological monitoring in emergency situations. URL https://www.iaea.org/newscenter/news/now-available-new-drone-technology-for-radiological-monitoring-in-emergency-situati

[15] Judith Perera. Monitoring drone developments in the nuclear sector. URL https://www.neimagazine.com/features/featuremonitoring-drone-developments-in-the-nuclear-sector-9610790/.

[16] Jerry A Towler. Autonomous aerial localization of radioactive point sources via recursive bayesian estimation and contour analysis.